VOL. 10, NO. 2 MAY 2000

SPIE's International Technical Group Newsletter

Electronic Imaging

Scanner sensor design to improve the color registration of image capturing devices

Scanners capture color images using three sensors: red (R), green (G), and blue (B). For most desktop scanners, this is accomplished using a 3-row CCD sensor. Each row is offset in the scanning direction by a few scan lines, and each row is responsible for capturing only one of the RGB colors. The captured data are recombined digitally to form a full 2D RGB image. Because the 3 rows of the CCD are separated in the scanning direction, the recombined RGB planes of the image do not necessarily align perfectly. The primary causes are due to optical aberration as well as scanner motion, and the resulting misalignment in color channels is referred to as color misregistration. The most familiar artifact is color fringing, which is most easily observed as false chromatic signals surrounding achromatic edges. However, with continuous tone images the most noticeable distortion as a result of misregistration is an increased luminance blur, due to the phase shift of the two most significant signals (R and G) contributing to luminance.

Since the early physiological structures of the visual system do not pass all the information in a displayed image to a percept, we consider the basic spatiochromatic behavior of the visual system as measured by psychophysics and modelled. The main behavior relevant to this application are the chromatic contrast sensitivity functions (CSFs) describing the visual sensitivity as a function of spatial frequency and color. While the CSFs for the red, green and blue stimuli[1] show differences in bandwidths (with blue being particularly reduced), the red and green CSFs are similar and do not suggest any technique for reducing the visibility of color fringing or the luminance blur resulting from their misregistration.

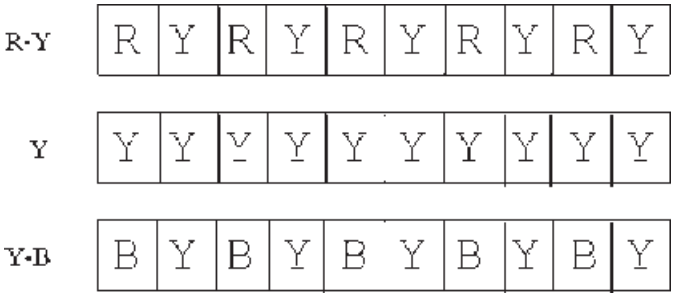

Figure 1. New sensor arrangement on the CCD focal plane.

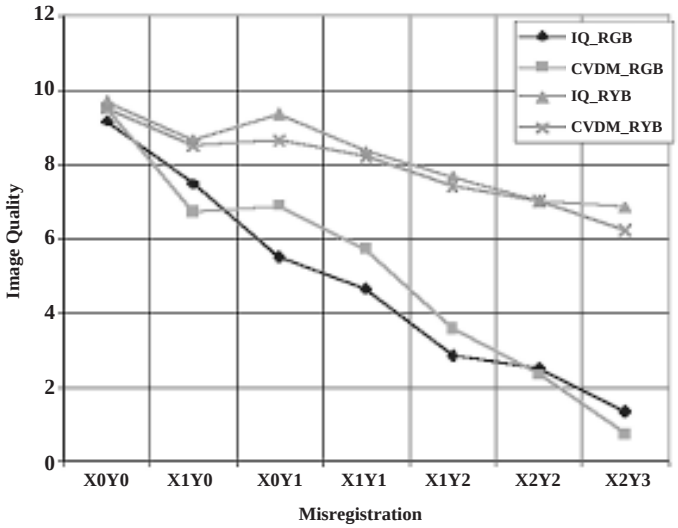

Figure 2. Image Quality scores from psychophysical experiment and CVDM.

However, if we consider the color representation at post-retinal locations in the visual system, the opponent color mechanisms suggest some interesting possibilities. Here there are three mechanisms formed from relatively simple combinations of cone signals having the important property that one has vastly superior bandwidths and peak sensitivity relative to the other two. The achromatic mechanism (Y) has the highest bandwidth and sensitivity, followed by an isoluminant green vs. red modulation (R/G), and with

continued on p. 3

Newsletter now available on-line

Beginning with this issue, Technical Group members will be offered the option to receive the Electronic Imaging Newsletter in an electronic format. An e-mail notice is being sent to all group members advising you of the web site location for this issue and asking you to choose between the electronic or printed version for future issues. If you have not yet received this e-mail message, then SPIE does not have your correct e-mail address in our database. To receive future issues of this newsletter in the electronic format please send your e-mail address to spie-membership@spie.org with the words ELECTRONIC IMAGING in the subject line of the message and the words "Electronic version" in the body of the message.

If you prefer to continue to receive the newsletter in the printed format, but want to send your correct e-mail address for our database, include the words "Print version preferred" in the body of your message.

Multiple digital display designs

Many display tasks require far greater display system capability than today's state-of-the-art systems provide. The human visual capability would ideally be the limiting factor in a display system. Economical system designs capable of generating eye-limiting visual acuity is indeed a challenge to the display industry. Future configurations will encompass multiple displays (as well as multiple display technologies within a single system), configured in a manner that allows the displays to be perceived as a single integrated image. Visual display technology is progressing rapidly beyond the traditional capabilities of the early industry workhorse the cathode ray tube. Configuring multiple displays (to perform as a video wall, a high-resolution display monitor, or a tiled display) will enhance performance as well as requiring designers to perform tradeoffs to compensate for a specific display technology's limitation.

Deficiencies in current direct view displays are best viewed in the context of "what humans are capable of seeing." Current direct view displays of VGA or greater resolution have a very limited dynamic range in gray scale, color depth, and resolution. In nature, light intensities vary from full sunlight—as seen during at clear mid day during the summer—to complete darkness. An ideal display would be able to vary in brightness between these two limits: a 10,000:1 dimming range. The dimming steps would be mapped to just noticeable differences with an over-sample reserve to allow for video-data-sampling quantization errors.

High bandwidth video data has to be transferred to the display without large latency. The minimum video rates require that the display be rendered at least 30 frames per second. The video data—having Mega-pixel resolution, 10,000:1 intensity dynamic range, contrast, grayscale, with greater color depth—will have to be transferred to the display simultaneously. Traditional data interfaces have been analog, although the display drivers sample this data to provide the grayscale or color depth data to the pixels. As resolution increases, the clock accuracy in the sampling (analog to digital) process become critical. Drift in the display clock or lack of synchronization with the image generator or graphic processor allows data to be lost (under-sampled for a given bandwidth). Additionally, the case has to be addressed where the displays are used in a non-native mode (display resolution or color depth set higher than the data being sent from the image generator). The display drivers sample the data afterwards, filling in the missing information according to a predetermined algorithm. The sampling designs should be viewed in the context of "how scaleable" they will be as we move toward the eye-limiting visual acuity of tomorrow's displays.

Digital displays offer different advantages compared to traditional analog displays. There are scaleability opportunities available when on-the-fly error correction is possible. The chief advantage of a digital display is the ability to quantize and control the data errors consistently and within a predefined tolerance. Many of the quantizing errors may be avoided or reduced by eliminating unnecessary intermediate conversions of data to analog and back to digital.

Since many digital displays are not inherently integrated with a particular light source or form of modulation, light valve technology may be interfaced with any one of a number of promising new light sources that are becoming more compact, bright, collimated, and polarization-controlled compared to earlier designs.

Digitization will offer many advantages over traditional analog display technology. Advantages of a totally digital display system include increased data compression, smart pixel updating, and a more effective use of the interface bandwidth. Techniques to increase the effective bandwidth include transferring only the data that has changed since the last frame. A bistable digital display allows only the pixels that have changed to be updated (regardless of the prior frame's pixel information). These digitized scanning techniques promise a higher data throughput as well as a reduction in the average display power. Smaller pixel feature size has been realized in analog displays, but digital displays, as they mature, will offer more accurate and efficient exhibition of information.

The challenge of achieving a display capability that significantly narrows the gap between eye-limiting acuity and current state-of-the-art electronic display technology will require a revolutionary approach to display design. Digitization of displays combined with open systems interface will play an important role in meeting this challenge. Many of the digital designs will evolve over time. New display technologies with higher resolution and color capability will require restructuring and redefining the video data transferred between the image generator, sensors and the displays. The change in the data structure, combined with the increase in the amount of data being transferred into the digital displays, will require a migration away from the traditional analog display interfaces. Many tasks that were traditionally localized will become increasing distributed across the data interface network as well as across multiple displays. As the distribution of video tasks among multiple displays increases, synchronization and data coherency issues will have to be managed, with visual-display-system-defined priorities.

Reginald Daniels
US Air Force Research Laboratory
Crew Systems Interface Division
AFRL/HECV
2255 H Street, Wright-Patterson AFB
OH 45433-7022
Phone: 937/255-8863 or 937/255-3671 x415
E-mail: Reginald.Daniels@WPAFB.AF.MIL

References

1. R. Daniels, *Multiple high definition digital displays*, **Proc. SPIE 395413,** 2000.
2. R. Daniels, *Realizing the increased potential of an open-system highdefinition digital projector design*, **Proc. SPIE 3634,** p. 171-179, 1999.
3. R. Daniels, *High definition displays for realistic simulator and trainer systems*, **Proc. SPIE 3363,** 1998.

Scanner-sensor design

continued from cover

an isoluminant blue vs. yellow modulation (Y/B) having the lowest performance. Considering that color misregistration problems usually result in a single layer with two layers offset from it in either direction, the properties of the opponent color system seem suited to the task.

Based on spatio-chromatic properties of the opponent model of color vision, we then develop a new strategy that combines sensor and algorithm design to reduce the perceptibility of the misregistration artifact. Figure 1 shows the new sensor arrangement. Instead of capturing R and B at the same resolution as luminance, the R and B are captured at half of the luminance resolution in the horizontal direction. Since the luminance signal is derived from one row of the CCD sensor, there is no blur caused by the misregistration the three rows. The chrominance signals (R-Y and B-Y) are also derived from the sensor response on their respective rows. Since there is no registration error between R and Y on the same row—besides the fixed shift due to the known interleaving in the horizontal direction—the false color signal around achromatic edges is eliminated.

The half-resolution RY and BY signals are first interpolated to full resolution using linear interpolation. The full-resolution interpolated R and Y (or B and Y) signals are sent to the color difference operator to derive the chrominance signals (R-Y and B-Y). The luminance-chrominance-chrominance (LCC) signals are converted to RGB for display or CMYK for printing. In most cases, image processing such as filtering, tone scale enhancement, etc are applied to the LCC image before it is displayed or printed.

Finally, we test the results of this strategy in two ways. The perceptibility of color misregistration is studied with both print simulations using observers as well as a color visual difference model (CVDM).[2] In the observer study, the effect of misregistration is simulated in software and printed on a printer. Observers judged the image quality (IQ) of the prints and assigned a score. In a separate study, the simulated images were input to a color visual difference model, which produces a visual difference map of spatio-chromatic Δ values. Comparison of the IQ scores from the psychophysical experiment and RMS Δ values from the CVDM model shows strong correlation with a correlation coefficient of 0.97. In Figure 2 are plotted both the image quality scores from the visual experiment and the model prediction. Both studies show that the new sensor arrangement reduces the perception of color misregistration significantly.[3]

Xiaofan Feng
Sharp Labs of American, Inc.
5750 NW Pacific Rim Blvd
Camas, WA 98607
Phone: 360/817-7569
E-mail: xfeng@sharplabs.com

References

1. G. J.C. van der Horst, C. M. M. de Weert, and M. Bouman, *Transfer of chromatic-contrast at threshold in the human eye*, **JOSA 57,** pp. 1260-1266, 1967.
2. E. W. Jin, X. Feng, and J. Newell, *The development of a color visual difference model (CVDM),* **Proc. IS&T PICS Conf.,** Portland, OR, p. 154, 1998.
3. X. Feng and S. Daly, *Vision-based strategy to improve the color misregistration of image capturing devices,* **Proc. SPIE 3969,** 2000.

3D display

continued from p. 4

2mm.

Next, a sequence of images of a colored 3D skull, generated from 3D computer tomography, were projected and the conditions where the projected 3D image was continuously observed were examined. It took about three seconds per frame to render images, as opposed to more than one hour per frame by the previous method. One could observe the 3D projected image with correct motion parallax at a distance of more than one meter from the system and within ten degrees, both horizontally and vertically, from the front of the display. Figure 2 shows that the motion parallax was reproduced.

Discussion

Because of the geometrical accuracy of projection and simplicity of design, this system has an advantage over other 3D display methods. As the quality of the projected 3D image is proportional to the resolution of LCD, the development of high-resolution LCDs will be essential to the practical use of this system. We intend to use this 3D display for surgical navigation system that superimposes 3D images on a patient via a half-mirror (see Figure 3).

Susumu Nakajima
Department of Orthopaedic Surgery
The University of Tokyo
7-3-1 Hongo, Bunkyo-ku
Tokyo, 113-8655, Japan.
Phone: +81-3-5800-8656
Fax: +81-3-3818-4082
E-mail: susumu@miki.pe.u-tokyo.ac.jp

References

1. M. G. Lippmann, *Epreuves reversibles donnant la sensation du relief,* **J. de Phys. 7** (4th series), pp. 821–825, 1908.
2. Y. Igarashi, H. Murata, and M. Ueda, *3-D display system using a computer generated integral photograph,* **Japan J. Appl. Phys. 17,** pp. 1683–1684, 1978.
3. S. Nakajima, K. Masamune, I. Sakuma, and T. Dohi, *Three-dimensional display system for medical imaging with computer-generated integral photography,* **Proc. SPIE 3957,** 24 January 2000.

Statistical techniques

continued from back cover

position of each edge point (*i.e.* each snake node) is followed automatically with time. It should be noted that the number of nodes defining the snake must be great enough for the result to be satisfying (see Figure 3).

Christine Bondeau, Elbay Bourennane, and **Michel Paindavoine**
Laboratoire LE2I
Universite de Bourgogne
UFR Sciences et Techniques
BP 47870
21078 Dijon cedex
FRANCE
Phone: +33 3 80 39 63 29
Fax: +33 3 80 39 59 10
E-mail: cbondeau@u-bourgogne.fr

References

1. D. L. Fried, *Optical resolution through a randomly inhomogeneous medium for very long and very short exposures,* **J. Opt. Soc. Am. 56** (10), pp. 1372-1379, 1966.
2. F. Roddier, *The effects of atmospheric turbulence in optical astronomy,* **Progress in optics XIX,** E. Wolf, North-Holland Publishing Company, Amsterdam, pp. 281-376, 1981.
3. C. Bondeau, E. Bourennane, and M. Paindavoine, *A principal component analysis based method for the simulation of turbulence-degraded infrared image sequence,* **Annals of Telecommunications 54** (5-6), pp. 324-330, 1999.
4. A. Vapillon, B. Collin, and A. Montanvert, *Appariement de contours 2D par analyse multirésolution hiérarchique de la déformation,* **16th Workshop on Signal and Image Processing (GRETSI)** (2), Grenoble, France, pp. 1291-1294, Sept. 1997.
5. O. Germain and Ph. Réfrégier, *Optimal snake-based segmentation of a random luminance target on a spatially disjoint background,* **Opt. Lett. 21** (22), pp. 1845-1847, 1996.

3D display system for medical imaging by computer-generated integral photography

Three-dimensional medical images are widely used for both diagnosis and surgery. Because three-dimensional anatomical structures should be grasped intuitively, it is desirable that they are displayed three-dimensionally.

3D display systems developed to date are classified into two categories, those using the principle of binocular stereoscopic vision (e.g., head-mounted displays), and those creating objects in a 3D space (e.g., realtime holography). With the former method, the depth of projected object is reproduced by the fixed binocular disparity of the images. Because the spacing of the observer's eyes is not always equal to that of lenses, the reconstructed 3D information in the observer's mind becomes inaccurate. It is difficult to reproduce motion parallax for many people at a time. Furthermore, visual fatigue is inevitable with this method. Consequently, systems based on binocular stereoscopic vision are not suitable for medical imaging.

The second method creates ideal 3D images that are suitable for medical imaging, but we believe it is too complicated to be used in medical applications.

We have developed a simple real-3D display system using the principle of integral photography (IP). IP was proposed by Lippmann[1] in 1908. It can record and reproduce 3D objects using just a lens array and photographic film. The principle of IP can be though of in terms of the transformation of 3D information into 2D coordinates, which is called computer-generated IP.[2] Despite its simplicity, IP has not been practically applied to 3D display for a long time, mainly because of the pseudoscopic image problem. Computer-generated IP could overcome this problem by hidden surface removal, but the cost of computation has prevented its practical application. To overcome such problems, we have devised a new, fast, 3D-rendering algorithm for computer-generated IP, and developed a 3D display system to work with it.

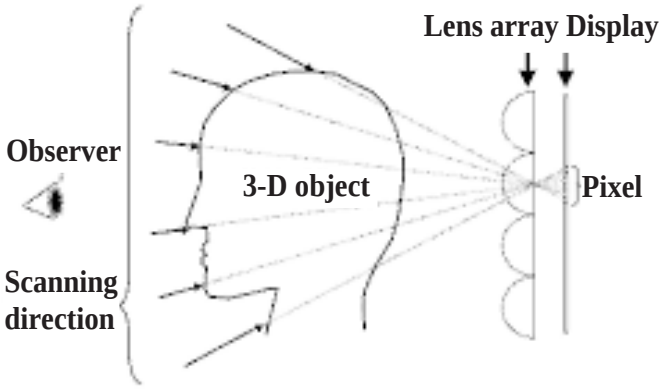

Figure 1. Schematic of a new, fast, 3D rendering algorithm for integral photography (IP). The line that occurs at the center of a pixel is extended through the center of the lens corresponding to that pixel. Then, the first point seen from the observer's side, where the line intersects the 3D object, is displayed on the pixel.

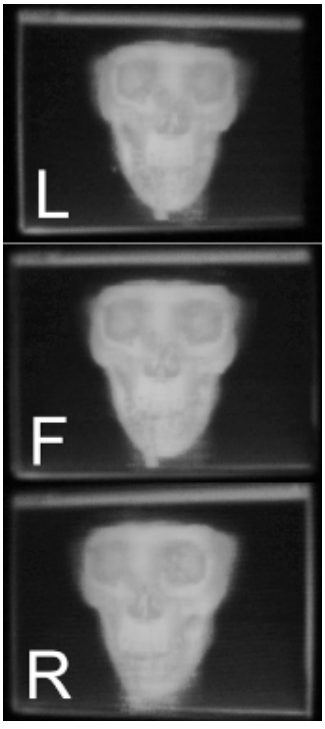

Figure 2. The photos of IP-projected 3D stationary skull images taken from front (F), left (L) and right (R).

Figure 3. (Top) Surgical navigation system as an application of the 3D display. Projected 3D internal structures of a patient are reflected by a half-mirror and superimposed on the patient. (Bottom) The operator can observe the reflected 3D internal structures (wrist bone) as if they could be seen through the patient's body.

Method

In the proposed computer-generated IP, each point in a 3D space is reconstructed by the convergence of rays from many pixels on the computer display through many lenses in the array. The observer can see any point in the display from various directions as if it were fixed in a 3D space: each point looks like a new light source. A 3D object can be reconstructed as an assembly of such reconstructed light sources.

Because LCD resolution is much lower than that of photographic film, the amount of information displayed decreases. Thus, only some of the points on a 3D object can be displayed on the LCD, and only the 3D information from the points most important to each pixel on the computer display must be processed. Only one coordinate of a point in the 3D object, corresponding to each pixel of the LCD, must be computed for each pixel on a display. We therefore devised a new, fast, 3D-rendering algorithm for IP that does this (see Figure 1). It can compute the point to be displayed for each pixel at a much faster speed than the previous method and performs hidden surface removal at the same time.

The LCD is used to display the image without distortion. The spatial location of the generated light source is decided by the diameter of the lenses on the lens array, the gap between lens array and the LCD, and the location of the pixel relative to the lens center.

Experiments

This system consists of a PC (Pentium2 dual), LCD (TFT, XGA, 106dpi), diffusive glass and hexagonal lens array (diameter=2.32mm).

Because geometrical accuracy is the most important parameter for medical imaging, the accuracy of projected point location at distances from 10 to 40 mm from the display were measured. The mean differences between the measured and the theoretical distances were less than

continued on p. 3

Differential image sequences for recovering 3D structure and camera motion from an uncalibrated camera

Our current work is focused on designing a real-time algorithm for estimating 3D structure and camera motion from a projected scene. We propose a practical method for achieving metric reconstruction from differential image sequences obtained with uncalibrated cameras.

Our approach can be divided into two main stages. First, the projection matrices between non-differential camera displacements are estimated. This process relies on the correct estimation of matched points. In order to efficiently deal with correspondence searches, a continuous differential tracking of selected points is accomplished by a real-time, probabilistic, parameter-estimation procedure. Making use of the resulting estimations, self-calibration and camera ego-motion estimation are carried out. In the second stage, a dense point reconstruction is performed, combining optical flow constraint with the projective model of a moving camera that has been determined previously.

In neither stage are correspondence searches found in an explicit way: rather, corresponding point searches are guided by a continuous tracking of selected points and optical flow constraint. Additionally, we implement a multi-resolution approach to avoid failures in employing differential models such as optical flow constraint: this is the case for large image displacements.

One of the main goals in machine vision is the recovery of spatial information about environment from the image-projected data. It is known that this process can be achieved from a sequence of images taken by a moving camera.[1] What kind of motion and additional constraints are essential to determine what level of recovery can be achieved. It becomes clear that, with an uncalibrated camera and no additional constraints, only projective reconstruction can be obtained from image correspondences. Hence the projection matrices and the reconstructed points can be obtained up to projective transformation.

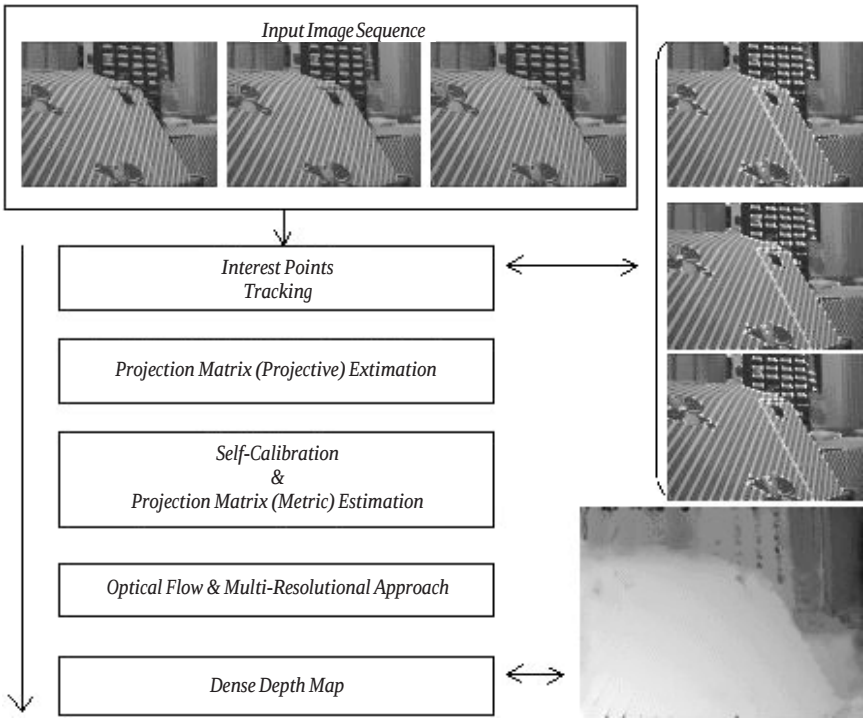

Figure 1. The system overview.

Figure 2. The estimated depth map at different levels of resolution.

To achieve metric reconstruction, it is necessary to have a calibration stage. This process fixes the plane at infinity at its original position and estimates the internal camera parameters, such as focal length, central points and skew.

Early work has fixed this problem using techniques of calibration based on using a patron jib, and knowledge of world-points that form this jib. The Maybank and Faugeras paper[2] opens up the a possibility of calibrating a camera by using a sequence of images, and without knowledge of scene points at which the camera is situated. In this kind of technique, the calibration process can be carried out with only the information available from the image sequence. Subsequent work has extended this process, allowing varying internal camera parameters.[3] Finally, in order to retrieve dense reconstructed points, a dense correspondence map must somehow be taken from the image sequence. This task can be accomplished by searches over epipolar lines and minimization criteria such as normalized cross correlation.[4]

Our current work differs from the latter approach in the method by which the matching points are obtained. As we are interested in real-time algorithms for scene reconstruction, this search must be less expensive than the former algorithm. Improvement in the time requirement can be achieved by taking advantage of differential image sequence properties. The key idea is to perform low cost calculations between differential images that are light enough that they can be carried out while camera is moving. In this way, to deal with the correspondence search, a continuous differential tracking of select points is accomplished by a real-time EM probabilistic estimation procedure. Secondly, a dense reconstruction process is performed combining optical flow constraint with the previously estimated projective model.

Overview of the method

The first step is to relate the different images. This is done by selecting a limited set of interesting points at the first frame, and by subsequently tracking them along consecutive differential images. In this process, it is assumed that these points are primarily chosen to be stable to rotational and translational movements. This process forms a set of continuous matching points that allow fundamental and projection matrix calculations between nonconsecutive

continued on p. 9

Method to significantly reduce the amplitude noise of a diode-pumped intracavity-doubled laser

Here we discuss a method of significantly reducing amplitude fluctuations of a laser beam from an intracavity-doubled laser. This is accomplished by modulating the pump to the laser gain medium in a specific way. The initial experiments consisted of sharply turning the pump laser off then on at a set frequency. This had the effect of reducing the optical noise from ~30% to <1%.

Intracavity-doubled lasers

The efficiency of the second harmonic generation (SHG) process increases with the incident intensity of the fundamental laser beam. Intracavity laser power is usually higher than the output beam power. These two facts motivate laser designers to place the SHG crystal inside the laser cavity along with the gain medium.[1] Under this condition, the laser cavity mirrors are usually chosen to reflect 100% of the fundamental light to keep the intracavity power as high as possible. The SHG crystal converts the circulating fundamental power to its second harmonic which is not reflected by the cavity mirrors. In order to send all the generated second harmonic light out in one beam, all the laser cavity mirrors (with the exception of the output coupler) are designed to also reflect 100% of the second harmonic wavelength.

A microchip laser exploits the intracavity doubling concept and couples to it large scale manufacturability and ease of use by the consumer. It is usually fabricated from two crystals (gain medium, SHG) attached together and polished such that their outside surfaces are parallel with each other. Appropriate optical coatings are placed on the outside surfaces of the crystals which subsequently define the laser cavity.[P1–P4] A diode laser "pump" provides the input energy. A diagram of a microchip laser is given in Figure 1 below.

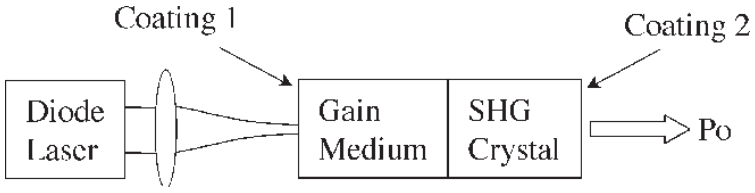

Figure 1. Diagram of an intracavity doubled microchip laser.

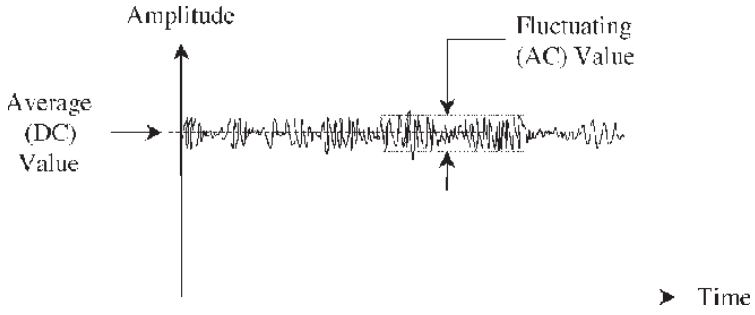

Figure 2. Method of noise amplitude measurement.

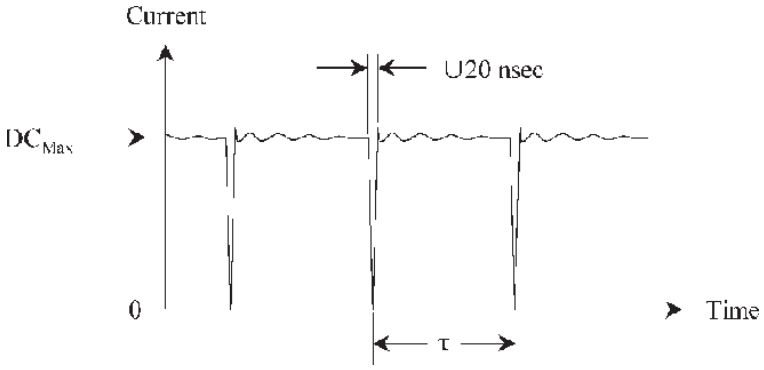

Figure 3. Current to the pump diode versus time.

Amplitude noise

The output beam from any laser will posses characteristics that are less than ideal. As an example, the output power from a continuous wave (CW) laser will fluctuate over time. One method of characterizing the amplitude noise of such a laser beam is shown in Figure 2.

A portion of the laser beam to be measured is directed onto a fast response DC-coupled photodetector. In a low noise signal, the AC component will be a very small proportion of the DC value.

Chaotic noise in intracavity-doubled lasers

Placing the SHG crystal and gain medium inside the same laser cavity couples together their two nonlinear processes (laser gain, SHG). The resulting system is highly nonlinear, unstable, and difficult to correct. Intracavity-doubled lasers typically suffer from large amplitude fluctuations, chaotic in time, in the output beam.[2,3] A great deal of effort has been dedicated to understanding and solving this dilemma.[4-6, P5–P11]

The solutions tend to deal with the fundamental laser design, can be difficult or expensive to implement, and are usually not easy to implement as a retrofit to an existing laser.

Chaotic noise reduction method

A very high frequency response pulsing circuit was designed and fabricated to drive the pump diode of a microchip laser producing blue light. The circuit produces a DC current which is pulsed to zero in very sharp "spikes" as illustrated in Figure 3 below.

Two conditions are necessary in order to make the laser operate in a quiet mode, the pulsing circuit has to be driving the pump diode, and an optimum temperature on the microchip laser is required which is not necessarily the optimum phase matching temperature. The noise of the output laser light (second harmonic), measured as described in Figure 2, is less than 1%. A typical result is shown in Figure 4.

The first experimental demonstration of this technique was conducted on 18 May 1999 in Aloha Oregon. This method is patent pending.

Ed Miesak
Laser Vision Technologies
10836 Glencove Circle, #208
Orlando, FL32817
Phone: 503/671-9792
Fax:503/356-8978
E-mail: ed_miesak@hotmail.com

continued on next page

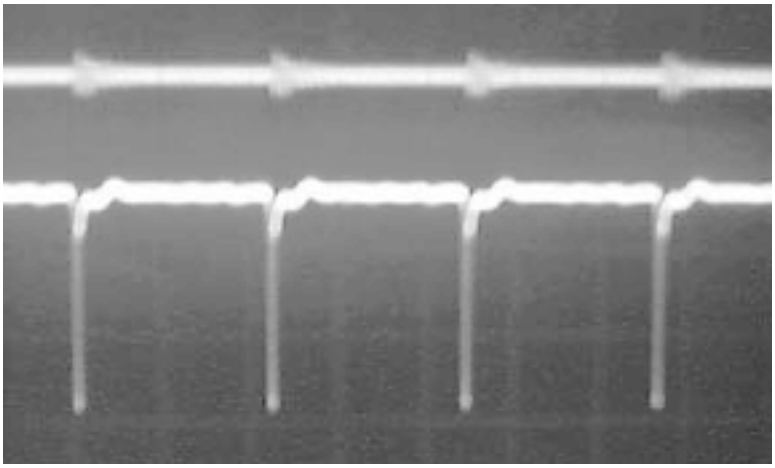

Figure 4. Oscilloscope trace of blue light (top) and the pump diode driving signal.

References

1. Richard G. Smith, *Theory of intracavity optical second-harmonic generation,* **IEEE JQE,** p. 215, April 1970.
2. T. Baer, L*arge-amplitude fluctuations due to longitudinal mode coupling in diode-pumped intracavity-doubled Nd:YAG lasers,* **J.O.S.A. B 3** (9), p. 1175, September 1986.
3. Glenn E. James, Evan M. Harrell II, Christopher Bracikowski, Kurt Wiesenfeld, and Rajarshi Roy, *Elimination of chaos in an intracavity-doubled Nd:YAG laser,* **Opt. Lett. 15** (20), p. 1141, 15 October 1990.
4. K. I. Martin, W.A. Clarkson, and D.C. Hanna, *Self-suppression of axial mode hopping by intracavity second-harmonic generation,* **Opt. Lett. 22** (6), p. 375, 15 March 1997.
5. M. Pierrou, F. Laurell, H. Karlsson, T. Kellner, C. Czeranowsky, and G. Huber, *Generation of 740 mW of blue light by intracavity frequency doubling with a first order quasi-phase-matched* $KTiOPO_4$ *crystal,* **Opt. Lett. 24** (4), p. 205, 15 February 1999.
6. Klaus Schneider, Stephan Schiller, Jurgen Mlynek, Markus Bode, and Ingo Freitag, *1.1-W single-frequency 532-nm radiation by second-harmonic generation of a miniature Nd:YAG ring laser,* **Opt. Lett. 21** (24), p. 1999, 15 December 1996.

Patents

P1. 5,610,934, *Miniaturized intracavity frequency-doubled blue laser,* 11 March 1997.
P2. 5,574,740, *Deep blue microlaser,* 12 November 1996.
P3. 4,731,787, *Monolithic phasematched laser harmonic generator,* 15 March 1988.
P4. 5,889,798, *Active switching laser and microchip laser,* 30 March 1999.
P5. 5,450,429, *Efficient linear frequency doubled solid-state laser,* 12 September 1995.
P6. 5,854,802, *Single longitudinal mode frequency converted laser,* 29 December 1998.
P7. 5,838,713, *Continuously tunable blue microchip laser,* 17 November 1998.
P8. 5,446,749, *Diode pumped multi axial mode intracavity doubled laser,* 29 August 1995.
P9. 5,638,388, *Diode pumped multi axial mode intracavity doubled laser,* 10 June 1997.
P10. 5,511,085, *Passively stabilized intracavity doubling laser,* 23 April 1996.
P11. 5,627,849, *Low amplitude noise intracavity doubled laser,* 6 May 1997.

The IRIS Laboratory: 3D imaging and data fusion at the University of Tennessee

The Imaging, Robotics, and Intelligent Systems (IRIS) Laboratory, in the University of Tennessee's Department of Electrical and Computer Engineering, performs research in three dimensional (3D) imaging and data fusion. Applications of this research include mapping of large facilities for robotic navigation, and automated construction of virtual environments for real time simulation. IRIS Lab core technologies are classified into the three areas illustrated in Figure 1 and described below.

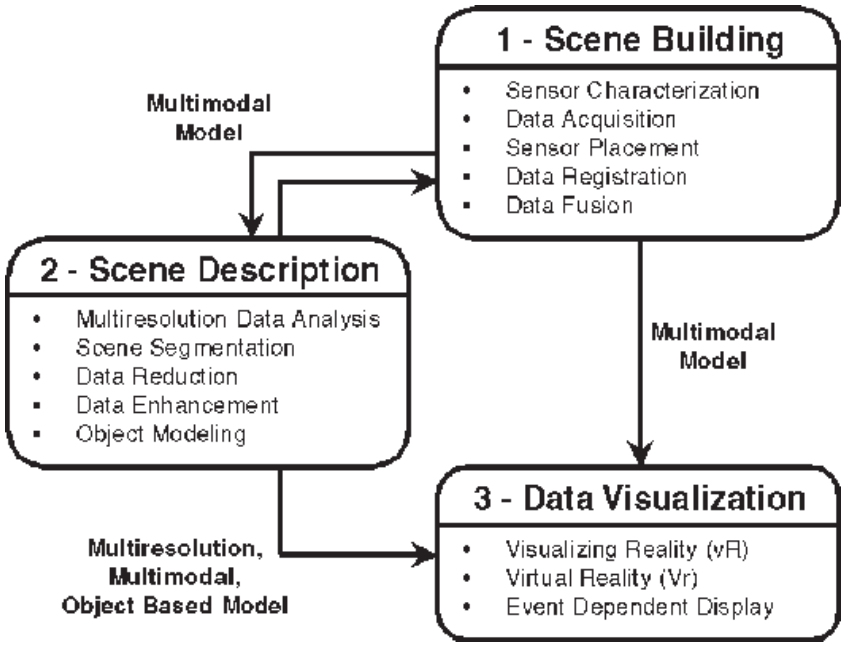

Figure 1. IRIS Lab core technologies.

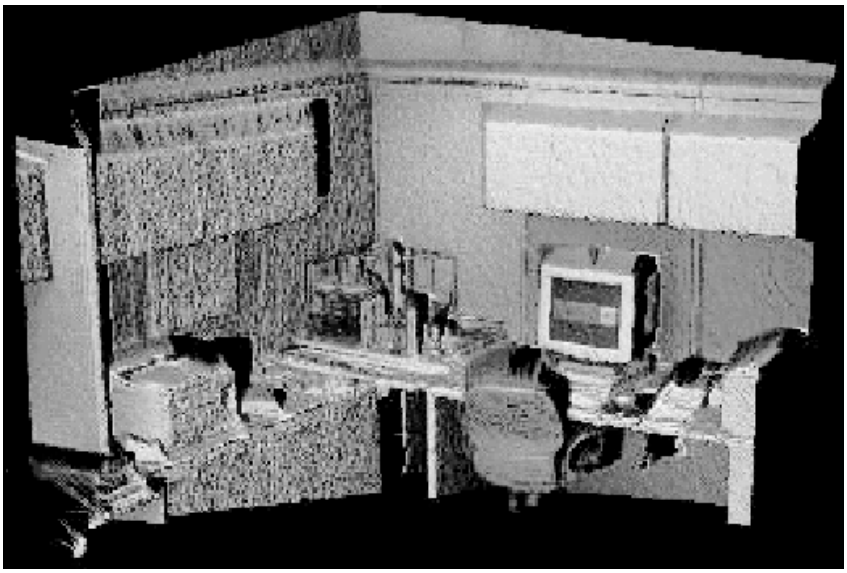

Figure 2. 3D scene automatically reconstructed from unregistered range and video.

Scene building

To acquire usable data, accurate sensor characterization is obviously important. In many scenarios, sensor placement must be addressed to ensure that the captured data is as accurate and as complete as possible. Data sets captured from different viewpoints, perhaps with different sensor modalities, must be registered to a common coordinate system. Once registered, the data can be fused to improve the information available from a single sensor, or to capture additional information, such as texture or thermal characteristics. The final outcome of this task is a dense lattice of 3D, multimodal data that describes the scene geometry and other spatial and spectral characteristics.

Scene description

Once constructed, a scene generally requires further processing to be of practical use. Objects of interest might need to be segmented from other objects, clutter, and/or background. After segmentation, objects may be modeled to aid in manipulation, recognition, and/or visualization. The amount of data captured in the scene building process often exceeds the needs or capabilities of the application, thereby necessitating data reduction. On the other hand, data enhancement may be required for the examination of small details. A multiresolution analysis of the data can benefit the solution of each of these problems. Referring to Figure 1, note that information flows in both directions between Scene Building and Scene Description. In many cases, intermediate scene description results can be used to modify the operation of the scene building module.

Data visualization

Current visualization activities are focused examining the results from scene building and scene description. As these results are often used for virtual reality (Vr) or to visualize reality (vR), research must account for varying visualization requirements. The objective is to provide appropriate data so that "event" dependent visualization can be achieved. Example events might include viewpoint, hardware limitations, constant frame rate, and/or object specific interest.

The IRIS Lab is presently supported by the U.S. Department of Energy (DOE) through the University Research Program in Robotics (URPR) and by the U.S. Army's Tank-automotive & Armaments Command (TACOM) through the National Automotive Center (NAC) and the Automotive Research Center (ARC).

continued on next page

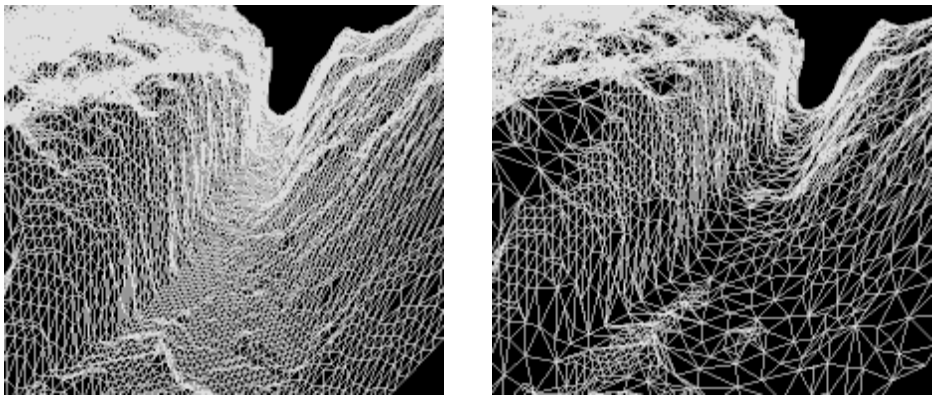

Figure 3. Mesh reduction using a multiresolution, wavelet analysis: (a) original terrain mesh; (b) mesh after reduction.

Mongi A. Abidi and **Jeffery R. Price**
328 Ferris Hall
University of Tennessee
Knoxville, TN 37996-2100, USA
E-mail: {abidi, jrp}@utk.edu
http://www.iristown.engr.utk.edu

References

1. C. Gourley, C. Dumont, and M. Abidi, *Enhancement of 3D models for fixed rate interactivity during display,* **Proc. IASTED Int'l Conf. Robotics and App.,** pp. 174-179, October 1999.
2. L. Wong, C. Dumont, and M. Abidi, *Next best view system in a 3D object modeling task*, **Proc. IEEE Int'l Symp. Computational Intelligence in Robotics and Automation:** CIRA'99, pp. 306-311, November 1999.
3. F. Boughorbal, D. Page, and M. Abidi, *Automatic reconstruction of large 3D models of real environments from unregistered data sets*, **Proc. SPIE 3958,** 2000.
4. H. Gray, C. Dumont, and M. Abidi,*Integration of multiple range and intensity image pairs using a volumetric method to create textured 3D models*, **Proc. SPIE 3966,** 2000.
5. E. Juarez, C. Dumont, and M. Abidi, *Object modeling in multiple-object 3D scenes using deformable simplex meshes*, **Proc. SPIE 3958,** 2000.
6. M. Toubin, D. Page, C. Dumont, F. Truchetet, and M. Abidi, *Multi-resolution wavelet analysis for simplification and visualization of multi-textured meshes*, **Proc. SPIE 3960,** 2000.
7. Y. Zhang, Y. Sun, H. Sari-Sarraf, and M. Abidi, *Impact of intensity edge map on segmentation of noisy range images*, **Proc. SPIE 3958,** 2000.

Differential image sequences

continued from p. 5

images. The position of these points is modelled by a probabilistic mixture of elemental densities, whose parameters are updated by the Expectation-Maximization algorithm for every new image that is acquired. In order to handle occlusion (appearance of new points and disappearance of old points), an extended version of this algorithm has been developed. This provides a natural way of continuously updating camera projection matrices.

Secondly, a calibration stage is carried out based on calculated projection matrices. This allows the retrieval of internal camera parameters along with camera position. To accomplish this, some qualitative assumptions about internal camera parameters need to be made, such as squared pixel, non-skew or fixed focal length. This self-calibration stage allows the recalculation of the projection matrices to those that have the plane at infinity as a reference plane.

Finally, a dense metric depth map is estimated, this stage is based on optical flow constraint along with metric projection matrices. To deal with larger displacements, a multi-resolution pyramid is employed, allowing a coarse to fine adjustment of depth estimations. As an example, Figure 1 shows the recovered depth map at different levels of resolution. The refinement process consists of using depth map calculations at lower resolutions as initial estimations for higher resolutions, and up through all pyramid levels.

In Figure 2 is shown the system overview. The algorithm has been implemented over an AMD K6-2 at 450Mhz. The code was developed in assembly language under the Linux operating system, and was allowed to incorporate MMX and 3Dnow instructions in critical integer and floating point calculations. In this environment, the speed was 200 megaflops and the frame reconstruction was performed at 3 frames/second.

Jose Vicente, D. Guinea, and **V. Preciado**
Instituto de Automática Industrial
Spanish Council for Scientific Research
La Poveda (Arganda del Rey)
28500 Madrid, Spain
E-mail: jvicente@iai.csic.es

References

1. R. Hartley, *Euclidean Reconstruction from Uncalibrated Views*, Proc. Second Europe-US workshop on Invariance, Ponta Delgades, Azores, 1993 (also published in Springer Lecture Notes, LNCS, 825).
2. S. J. Maybank and O. D. Faugeras, *A theory of self-calibration of a moving camera*, **Int'l J. of Comp. Vision 8,** pp. 123-152, 1992.
3. M. Pollefeys, R. Koch, and L. Van Gool, *Self-Calibration and Metric Reconstruction in spite of Varying and Unknown Internal Camera Parameters*, **Int'l J. of Comp. Vision 32** (1), pp. 7-25, 1999.
4. R. Koch, **Automatische Oberflächenmodellierung starrer, dreidimensionaler Objekte aus stereoskopischen RundumAnsichten,** Ph.-D. Thesis, Universität Hannover, September 1996.

CALENDAR

2000

Sixth International Conference on Remote Sensing for Marine and Coastal Environments

1-3 May
Charleston Area Convention Center
Charleston, South Carolina USA
SPIE is a cooperating organization. Sponsored by ERIM. Contact: EI/Marine Conferences, PO Box 134008, Ann Arbor, MI 48113-4008 USA. Phone: (1) 734/994-1200 ext 3234. Fax: (1) 734/994-5123. Email: wallman@erim-int.com. Web: www.erim-int.com/CONF/marine/MARINE.html.

SID Symposium 2000

14-19 May
Long Beach, California USA
Contact: Society for Information Display, 1526 Brookhollow Dr., Ste. 82, Santa Ana, CA 92705-5421 USA. Phone: (1) 714/545-1526. Fax: (1) 714/545-1547. E-mail: socforinfodisplay@mcimail.com. Web: www.sid.org

Visual Communications and Image Processing

20-23 June
Perth, Australia
For more information, contact SPIE at spie@spie.org.

Optical Science and Technology

SPIE's Annual Meeting
30 July-4 August
San Diego Conv. Ctr., San Diego, California USA
Technical Exhibit: 1-3 August

24th International Congress on High Speed Photography and Photonics

25-29 September
Sendai, Japan
SPIE is secretariat for this and will publish proceedings. For more information contact: Prof. Kazuyoshi Takayama, Tohoku Univ., Institute of Fluid Science, Shock Wave Research Ctr. 2-1-1 Katahira Aoba, Sendai 980-77 Japan. Phone: 81-22-2175283. Fax: 8122-2175324. E-mail: takayama@ifs.tohoku.ac.jp.

EUROPTO® Series Symposium on Remote Sensing

25-29 September
Barcelona Sants Hotel, Barcelona, Spain
Abstract due date: 28 Feb. 2000. Cosponsored by SPIE and European Optical Society.

For More Information Contact

SPIE • PO Box 10, Bellingham, WA 98227-0010
Phone (1) 360/676-3290 • Fax (1) 360 647-1445
E-mail spie@spie.org • Web www.spie.org

International Symposium on Remote Sensing of the Atmosphere, Environment, and Space

9-12 October
Sendai, Japan

Photonics East

5-8 November
Boston, Massachusetts USA
Including international symposia on:
- **ISAM '00—Intelligent Systems and Advanced Manufacturing**
- **VVDC '00—Voice, Video, and Data Communications**
- **EIS '00—Environmental and Industrial Sensing**

Technical Exhibit: 6-8 November

2001

Photonics West

19-26 January
San Jose Conv. Ctr., San Jose, California USA
Including international symposia on:
- **LASE '01—High-Power Lasers and Applications**
- **OPTOELECTRONICS '01—Integrated Devices and Applications**
- **BiOS '01—International Biomedical Optics Symposium**
- **SPIE/IS&T's EI '01—Electronic Imaging: Science and Technology.**

Education Program and Short Courses;
Technical Exhibit.

Join the SPIE/IS&T Technical Group

...and receive this newsletter

This newsletter is produced twice yearly and is available only as a benefit of membership in the SPIE/IS&T Electronic Imaging Technical Group.

IS&T—The Society for Imaging Science and Technology has joined with SPIE to form a technical group structure which provides a worldwide communication network and which is advantageous to the memberships of both societies.

Join the Electronic Imaging Technical Group for US$30. Technical Group members receive these benefits:

- *Electronic Imaging* Newsletter
- SPIE's monthly newspaper, *OE Reports*
- annual list of Electronic Imaging Technical Group members
- discounts on registration fees for IS&T and SPIE meetings and on books and other selected publications related to electronic imaging.

Persons who are already members of IS&T or SPIE are invited to join the Electronic Imaging Technical Group for the reduced member fee of US$15.

Please Print ☐ Prof. ☐ Dr. ☐ Mr. ☐ Miss ☐ Mrs. ☐ Ms.

First (Given) Name _____ Middle Initial _____

Last (Family) Name _____

Position _____

Business Affiliation _____

Dept./Bldg./Mail Stop/etc. _____

Street Address or P.O. Box _____

City _____ State or Province _____

Zip or Postal Code _____ Country _____

Phone _____ Fax _____

E-mail _____

Technical Group Membership fee is $30/year, or $15/year for full SPIE and IS&T Members.

Amount enclosed for Technical Group membership **$** _____

❑ **Yes! I want to subscribe to IS&T/SPIE's *Journal of Electronic Imaging* (JEI)** **$** _____
(see prices below)

Total $ _____

❑ **Check enclosed.** Payment in U.S. dollars (by draft on a U.S. bank, or international money order) is required. Do not send currency. Transfers from banks must include a copy of the transfer order.

❑ **Charge to my:** ❑ **VISA** ❑ **MasterCard** ❑ **American Express** ❑ **Diners Club** ❑ **Discover**

Account # _____ Expiration date _____

Signature _____
(required for credit card orders)

JEI 2000 subscription rates (4 issues):	**U.S.**	**Non-U.S.**
Individual SPIE or IS&T member	$ 50	$ 50
Individual nonmember and institutions	$215	$235

Your subscription begins with the first issue of the year. Subscriptions are entered on a calendar-year basis. Orders received after 1 September 2000 will begin January 2001 unless a 2000 subscription is specified.

Send this form (or photocopy) to:
SPIE • P.O. Box 10
Bellingham, WA 98227-0010 USA
Phone: (1) 360/676-3290
Fax: (1) 360/647-1445
E-mail: membership@spie.org

Please send me:
☐ **Information about full SPIE membership**
☐ **Information about full IS&T membership**
☐ **Information about other SPIE technical groups**
☐ **FREE technical publications catalog**

Electronic Imaging

The *Electronic Imaging* newsletter is published by SPIE—The International Society for Optical Engineering and IS&T—The Society for Imaging Science and Technology. The newsletter is the official publication of the International Technical Group on Electronic Imaging.

Technical Group Chair	Arthur Weeks
Technical Editor	Sunny Bains
Managing Editor/Graphics	Linda DeLano
Advertising Sales	Roy Overstreet

Articles in this newsletter do not necessarily constitute endorsement or the opinions of the editors, SPIE, or IS&T. Advertising and copy are subject to acceptance by the editors.

SPIE is an international technical society dedicated to advancing engineering, scientific, and commercial applications of optical, photonic, imaging, electronic, and optoelectronic technologies.

IS&T—The Society for Imaging Science and Technology is an international nonprofit society whose goal is to keep members aware of the latest scientific and technological developments in the fields of imaging through conferences, journals and other publications.

SPIE—The International Society for Optical Engineering, P.O. Box 10, Bellingham, WA 98227-0010 USA. Phone: (1) 360/676-3290. Fax: (1) 360/647-1445. E-mail: spie@spie.org.

IS&T—The Society for Imaging Science and Technology, 7003 Kilworth Lane, Springfield, VA 22151 USA. Phone: 703/642-9090. Fax: 703/642-9094.

Want it published?

Submit work, information, or announcements for publication in future issues of this newsletter by e-mail to Sunny Bains at sunny@spie.org, or at the address above. Articles should be 600 to 800 words long. Please supply black and white photographs or line art when possible (figures are also accepted electronically via FTP by SPIE in TIFF and GIF formats). Permission from all copyright holders for each figure and details of any previous publication should be included. All materials are subject to approval and may be edited. Please include the name and e-mail address of someone who can answer technical questions. Calendar listings should be sent at least eight months prior to the event.

Statistical techniques for the restoration of images degraded by atmospheric turbulence

Atmospheric turbulence has perturbing effects on high-resolution imaging. The optical refractive index undergoes random fluctuations in such a turbulent medium. This disturbs light propagation and the obtained image quality can be very poor depending on meteorology and exposure time.[1,2]

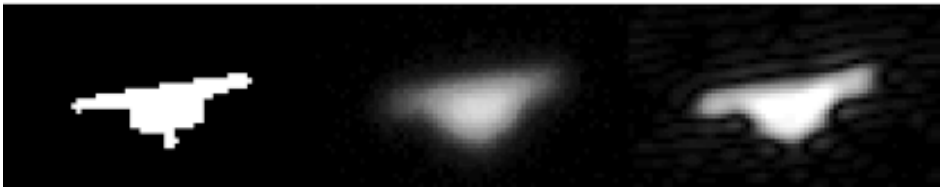

Figure 1. Left: object. Center: long-exposure (LE) image. Right: restored LE image (Wiener filter).

Figure 2. Part of an image sequence.

Figure 3. Left: example of partition into a set of subregions. Center: restored image, region-based approach. Right: restored image, edge-based approach.

We intend here to improve the quality of images of an object lying at 15 to 20km from a video camera. The light propagates horizontally, near the Earth's surface. The wavelength used is in the infrared band, because perturbations are weaker here than in the visible. Our images thus have high contrast. Despite the high resolution (25 μrad per pixel), the object appears quite small (about 30×30 pixels).

The existing turbulence-degraded image restoration techniques are usually dedicated to astronomy (adaptive optics), where they need to know the instantaneous random atmospheric point-spread function or use a wavefront sensor (speckle interferometry, wavefront-analysis-based deconvolution). Our goal is to recover the real shape of the object only from its degraded long-exposure (LE) or short-exposure (SE) images.

On a LE image, the object is blurred and the corresponding transfer function can be estimated if both the atmospheric conditions and the optical characteristics of the camera are known. However, restoring the image with classical deconvolution filters (Wiener filter, Tikhonov or Laplacian regularization) does not provide an accurate estimation of the object (see Figure 1): details are lost, both because of small object size and the low-pass filtering of the atmosphere. On the other hand, part of the high frequency component remains in an SE image up to the cut-off frequency of the camera. Thus it is better for us to work with SE images.

Our infrared camera can record sequences of a few tens of images at a video frequency of 100 Hz. The short integration time (lower than turbulence lifetime) gives sharp object edges. The degradation is here mainly due to anisoplanatism: the object shape fluctuates randomly (see Figure 2). The degraded images presented here were obtained using a complete simulation method that produces SE image sequences.[3]

Random object deformation requires a statistical processing of the received images. We propose two different approaches. First is the region-based approach where each image is partitioned in a fixed number of subregions, which are characterized both by their total intensity and by the shape of the object detail they contain. For a sequence of subregions at a given place in the field of view, the most probable one, in a statistical sense, is the closest to the average subregion. This way we can recover a good estimation of the original object (see Figure 3).

Second is the edge-based approach where, through a Bayesian analysis, we show that the optimal estimate (in the maximum-likelihood sense) of the object edge is given by the average position taken by edge points, which implies the following of each edge point position through the sequence.

Matching point to point, each pair of consecutive contours with a multiscale algorithm[4] gives quite satisfying results. However this method is very sensitive to the least matching error—leading rapidly to a smoothing of details—because of the small number of pixels in the object.

It seemed to us more convenient to use statistical, region-based active contours (snakes). The image has only two, highly contrasted, regions (object and background), so each pixel can be considered as a random variable, described by a Bernouilli law. The optimal region-based snake[5] converges well onto the object edges in the first image. Afterwards, it follows the object deformations through the sequence. Here the

continued on p. 3

SPIE Society of Photo-Optical Instrumentation Engineers

P.O. Box 10 • Bellingham, WA 98227-0010 USA

Change Service Requested

DATED MATERIAL

Non-Profit Org.
U.S. Postage Paid
Society of
Photo-Optical
Instrumentation
Engineers